I&EC research
Industrial & Engineering Chemistry Research

Article

Optimization of an UV-Induced Graft Polymerization of Acrylic Acid on Polypropylene Films Using CdS as a Light Sensor

María Fernanda Stragliotto, Miriam C. Strumia, Cesar G. Gomez, and Marcelo Ricardo Romero

Ind. Eng. Chem. Res., **Just Accepted Manuscript** • DOI: 10.1021/acs.iecr.7b04526 • Publication Date (Web): 04 Jan 2018

ACS Publications

Industrial & Engineering Chemistry Research is published by the American Chemical Society. 1155 Sixteenth Street N.W., Washington, DC 20036

Optimization of an UV-Induced Graft Polymerization of Acrylic Acid on Polypropylene Films Using CdS as a Light Sensor

María Fernanda Stragliotto[1, 2], Miriam C. Strumia[1, 2], Cesar G. Gomez[1, 2,*], Marcelo R. Romero[1, 2]

[1] *Departamento de Química Orgánica, FCQ-UNC. Edificio de Ciencias II. Haya de la Torre y Medina Allende. (5000) Córdoba, Argentina.*

[2] *Instituto de Investigación y Desarrollo en Ingeniería de Procesos y Química Aplicada (IPQA), CONICET, (5000) Córdoba, Argentina.*

Abstract

Photoconductive cell of CdS was used to optimize the photograft polymerization of acrylic acid (AA) onto polypropylene film surface. Effect of UV-light intensity on the performance of this reaction in the three-dimensional space inside the reactor was researched. A relationship between light intensity measured as conductance and performance of AA graft reaction was found. In addition, a linear relationship (r^2 = 0.98) between grafting degree (G) and conductance (G / wt.% = (2.2 ± 0.1) 10^4c - (0.3 ± 0.4)) was determined in the range 5 to 20% G, where a minimum stabilization time such as 5 minutes was required. Standard deviation of G value and conductance decreased when longer distance between the film and the lamp was used, leading to a more homogeneous surface modification. Therefore, we propose this system as a new method to monitor and predict the performance of UV-induced reactions.

* Corresponding author. Tel.: +54-0351-535-3867 Annex 53343.
E-mail addresses: gom@fcq.unc.edu.ar

Keywords: *UV LIGHT, GRAFTING, POLYPROPYLENE, PHOTOGRAFT, FILM, SURFACE, PHOTOCONDUCTIVE, CADMIUM SULPHIDE.*

1. Introduction

Design and generation of new polymeric materials containing a specific structural organization, together with a particular functionality, are of great interest in materials technology.[1-6] These materials can be achieved by adjusting the chemical composition of their bulk or after surface modification of a given support.[7-12] As an example, a synthetic polymer like polypropylene (PP) has been widely used due to its mechanical properties, chemical resistance and ability to act as a barrier for certain gases.[13-15] However, several modification reactions have taken place on PP to improve its properties. A special case is superficial modification by using UV light like a strategic process to obtain films for different applications.[13, 16-19] Therefore, these materials can be modified with tailored surface properties without altering their bulk features.[20] However, for these systems, several reaction conditions need to be previously set; thus, the study often becomes cumbersome. Although there are a lot of studies where the support surface has been modified by using an UV-induced reaction,[21-24] there is generally little information about the effect of light power on the reaction performance.[25] Therefore, in this work we researched the effect of the reaction mixture position about light source and the reaction time on the performance of a photograft polymerization. Surface of PP films was modified by using an UV-induced graft polymerization of acrylic acid (AA), selected as a reaction model.[13, 16, 26] It is known that the distance between light source and reaction mixture is a crucial variable for this kind of reaction.[27] In order to monitor the changes of lamp light intensity against the variables mentioned above, we used a photoconductive cell of CdS as a light sensor.[28-30] Benzophenone was used as a radical photoinitiator agent in an aqueous reaction mixture containing AA.[31] After having acquired data of the grafting degree of poly acrylic acid grafted onto the surface of PP film for different reaction conditions, a mathematical expression was proposed to correlate the performance of this reaction against light intensity.

2. Experimental

2.1 Reagents and methods

In most cases the reagents were used as purchased. Isotactic PP film with a thickness of 20 μm was kindly supplied by Converflex S.A., Argentina. Crystallinity degree (48 %) was determined from the melting endotherm of the polymer measured with a Perkin-Elmer Pyris DSC calorimeter at a heating rate of 10 °C.min^{-1}. AA, p.a. grade (Sigma-Aldrich, USA). Benzophenone (BP) p.a. grade (Mallinckrodt, USA).

2.2 Configuration of measurement system for UV radiation

A simple data acquisition system was developed to record the intensity of an UV radiation (254 nm) generated from a lamp, with a length of 25 cm (NNI 40/20 35W, UV-Consulting Peshl®, Spain), centered on the top of a reactor camera together with a photoconductive cell of CdS (Model#3190 SUNROM, India) used as a sensor of light intensity (Figure 1). The photoconductive cell of CdS, commonly named light dependent resistance (LDR), was placed in a 4 x 3 x 3 cm plastic box with a sensitive face exposed to a 2 mm circular aperture of diameter.[32] It was then covered with a transparent quartz glass of optical quality to allow passage of ultraviolet light beam. LDR sensor was located at different positions inside the reactor box and exposed to UV radiation (Figure 1). LDR was connected to the terminals of a digital multimeter (UNIT60, USA), which has an optical interface. The data registered were sent to a computer via serial port (0378h) and stored (.dat) using a data acquisition software, which was supplied by the multimeter manufacturer. The software was set to record ohmic resistance for each second during the time required to complete the assay.

Figure 1

2.3 Study of the spectral sensitivity of the LDR sensor

In order to study the spectral sensitivity of the LDR sensor, an UV-visible spectrophotometer (Shimatzu UV-1800, UV Probe 2.3, Japan) was used. A light emitter diode (LED) with an emission wavelength at 550 nm (red) was used to excite one of the spectrophotometer detectors with a constant light intensity powered by a circuit of 20 mA - 5V. Another detector was used to determine the intensity (I_e) emitted by source from the lamps of the spectrophotometer at different wavelengths (200-900 nm), where the signal obtained was registered as absorbance (Abs). Therefore, under these experimental conditions, the absorbance was reciprocal to the estimated intensity of the lamp ($I_e \propto Abs^{-1}$) at each wavelength recorded. Subsequently, the LDR sensor was placed in the path of the light beam at different wavelengths and the resistance (Ω) of the sensor during spectral sweeping was recorded. The resistance measured was expressed as conductance (c) and its value corrected (c´) with the I_e value at different wavelengths (c´ / S = c x Abs). The spectral sensibility (ss) was calculated as in the following expression:

$$ss/\% = 100 \times \frac{c'}{c'_{max}} \quad (1)$$

where the parameter c'_{max} corresponds to the highest c´ value of emitted light for the spectral curve. The results obtained were compared with those ss values provided by the manufacturer of the LDR.[32]

2.4 Response time of the LDR sensor exposed to UV light

LDR sensor was placed inside the reactor under UV lamp to study its response time. The quartz window of the sensor was covered with a black surface associated to a stepper motor. A half rotating disc enabled passage of the light beam at a given frequency (Figure 2). The stepper motor was connected to a driver circuit (based on NPN Darlington switch ULN2068B, ST Microelectronics, Switzerland) and controlled by a microcontroller (Arduino UNO ATmega328,

Italy). A simple program controlled the position of the motor, which periodically allowed or not passage of UV light to the LDR sensor. The experiment started when the UV lamp was turned on, reaching stabilization of light intensity near 8 minutes. The sensor was periodically covered or not by the black surface each 12 s. The time required to reach maximum sensitivity once the sensor was exposed to the light beam was less than 1 s, repeating this cycle 30 times. The sensor response was recorded and compared with data provided by the manufacturer for other wavelengths.

Figure 2

2.5 Performance of UV light intensity as a time function during lamp ignition

In this study, the LDR sensor was placed into the reaction camera at the position D, H and W from the lamp, corresponding to 7, 12 and 24 cm, respectively. The lamp was lit, and its light emission was cut with an opaque surface for 480 s to reach the stabilization of the light intensity. After that, the opaque surface was removed and the UV intensity as a time function was recorded as conductance in a continuous mode by the LDR sensor. This assay was repeated five times at different days to compare the ignition of the lamp at room temperature. After each experiment, the lamp was turned off and its temperature was equilibrated after 6 h at room temperature.

2.6 Performance of UV light intensity inside the reaction camera

Intensity of emitted UV light as a function of lamp stabilization time with LDR sensor was recorded. Figure 3 shows a three-dimensional reactor image where four study levels (A, B, C and D) were found, corresponding to 4, 12, 20 and 28 cm from the UV lamp, respectively.

Figure 3

Figure 3 shows the dots for each level, which represents the position where the LDR sensor was placed into the reaction camera to measure light intensity distribution. In addition, the cylindrical structure on top of the reactor marks the position of the ultraviolet light source.

2.7 Grafting reaction on PP films and their characterization

2.7.1 Preparation of polymeric films and AA-photograft polymerization

Surface of PP films was modified by photograft polymerization of AA. Previously these films were cleaned with ethanol and then dried at room temperature until reaching constant mass. Then, we added 10 mL of a reaction mixture (RM) containing benzophenone (0.2 M) and AA (3 M) solubilized in water, used as photo-initiator agent and monomer, respectively. AA-photograft polymerization was performed as follows: the surface of a dried film was left in contact with RM over a flat glass using a ratio of 168 cm^2 of film surface area per mL of RM. The PP-RM-glass system (from top to bottom) was then exposed to UV light at different times and positions inside the reaction chamber. Finally, each film was exhaustively washed with 1 M of NaOH and then with 1 M of HCl aqueous solution and distilled water. Modified PP films were dried at 50° C until reaching constant mass. The degree of polyacrylic acid (PAA) grafted (G) onto PP film was calculated from Equation 2, where PP and PP-PAA represent the initial and the final film mass, respectively.

$$G/wt.-\% = \left(1 - \frac{PP}{PP - PAA}\right).100 \quad (2)$$

2.7.2 FT-IR Spectroscopy of PP films

In addition, the initial PP and modified PP film were superficially characterized by FT-IR Spectroscopy. Attenuated Total Reflectance (ATR) spectra were recorded with a Thermo Scientific Nicolet iN10 FTIR spectrometer. A zinc selenide ATR crystal at 45° was used in a

wavenumber range of 4000 to 600 cm^{-1} at 4 cm^{-1} resolution for 16 scans with Omnic 8 (Nicolet) data processing.

2.7.3 Contact angle measurements

The measurements were performed using a homemade contact angle goniometer by the Sessile Drop method at 20°C. A micro-syringe was used to measure water drops of (4.00 ± 0.04) mm^3 and dropped from (2.00 ± 001) mm to the surface of the film. During this procedure, a video was made using a CMOS digital camera. Each video was processed using SPANISH-DUB software; in all cases, the frame obtained 5 s after the drop lay onto film surface was selected. The frame capture was processed with IMAGEJ 1.4g software. All assays were performed in quintuplicate measuring three different places of each sample.

2.7.4 Film thickness determination

The thickness of films at several locations was determined at least 5 times by using a thickener (Schwyz, Switzerland). All measurements were performed at 20 °C.

2.7.5 Effect of film position on the performance of grafting reaction

PP films were placed in contact with RM following the method described in the experimental section. AA-photograft polymerization was studied at four different levels such as A, B, C and D as shown in Figure 4. Dots delimit the perimeter of 4 films for each level, positioned at 15, 21, 27 and 33 cm of width. This assay was performed three times for a given reaction condition, where a rectangular film (6 x 10 cm) was used. Photoluminous reaction was started 8 min after turning on the UV lamp when the system PP-RM-glass was exposed to UV light for 120 s. Subsequently, the film was washed and dried.

Figure 4

2.7.6 Effect of lamp stabilization on the yield of grafting reaction

Effect of stabilization time of light intensity on the performance of AA-photograft polymerization onto PP films was carried out. Figure 5 shows the position of a rectangular film (14 x 20 cm) used in this assay whose perimeter is indicated from four points at the level C. A stabilization time at 0, 2, 4, 6, 8, 10 or 15 min after turning on the light source was investigated. In this assay, the PP-RM-glass system was exposed to the lamp light for 120 s. During stabilization time, the PP-RM-glass system was protected from UV light with an opaque surface. Each reaction condition was analyzed at least three times.

Figure 5

3. Results and discussion

3.1 Study of spectral curve and response time of LDR sensor

The ss value of the LDR sensor was studied against a light of different wavelengths. Figure 6 shows the ss value recorded by the sensor as a function of the wavelength, where it can be observed that the highest sensitivity (ss_{max}) of the sensor is around 600 nm. In addition, the spectral response and the maximum sensitivity found for the LDR sensor were similar to those informed by the manufacturer of this device.[32] However, no information could be found on the sensitivity of this kind of sensor for ultraviolet light region. Therefore, in this experiment the ss parameter at 254 nm (ss_{254}) was determined with the LDR sensor, showing a ss_{254} value near 7.3 %, as seen in the inset of Figure 6.

Figure 6

Since the temporal response of the emission of the UV light source must be studied, the response time of the LDR sensor needs to be previously known. Manufacturer reports a typical

rise and fall time (10 lux) of 18 and 120 ms, respectively. However, it was not evaluated for a range of ultraviolet light. Figure 7 shows the response of the LDR sensor in the presence or absence of UV light versus time. In all cases it was observed that the LDR sensor reached a stabilized c_{254} value close to 0.8 mS with a response time near 1 s or less.

Figure 7

Although a shorter time can be determined by the LDR sensor for UV light, data acquisition system has a recording time longer than 1 s (Figure 2). Under the presence or absence of UV light, a repetitive response of the LDR sensor was found. All measurements were made with a lamp previously stabilized for at least 8 min.

3.2 Response of emitted ultraviolet light as a time function during lamp ignition

Figure 8 shows conductance variation after the ultraviolet lamp was turned on. At the beginning, conductance increased fast, showing an intense peak with 1 s of duration after ignition. Then, conductance increased its value three times, reaching a plateau after 5 min. For further analysis, the temporal response of the lamp was adjusted using a sigmoid function as in Equation 3:

$$\frac{C_{254}}{C_{\infty}} = \left[\frac{(1 - C_0)t^3}{t_{1/2}^3 t^3}\right] + C_0 \qquad (3)$$

where C_{254} is the conductance at a given time t, while C_∞ is the conductance at infinite time, the ratio of $C_{254}.C_\infty^{-1}$ being called normalized conductance; C_0 = 0.3 is a basal conductance produced by the lamp for few seconds after being turned on. In addition, parameter $t_{1/2}$= 2 is the time required to achieve the following equation, where $C_{254}\ C_\infty^{-1} = 1 - C_0$. Figure 8 exhibits the

adjustment of the experimental data from the use of Equation 3, with a determination coefficient of 0.98. Lamp response could be properly predicted from the use of this model. Figure 8 shows that the normalized conductance mostly changes during the first 300 s after turning on the lamp, which has a strong influence on the reaction kinetics as well as on the performance of the grafting reaction. Clearly, the response measurement of light source provides a quantitative tool to determine an adequate time to stabilize the light source.

Figure 8

Considering the data shown above, where the intensity of the ultraviolet light is a function of lamp ignition time, this phenomenon may be associated with the fact that such ignition time variation influences the yield of grafting reaction. Therefore, the relationship between the stabilization time of lamp and the G value must be analyzed. In addition, other authors already studied the performance of photograft polymerization onto film surface versus reaction time, describing a similar tendency to that shown in Figure 8.[16, 33, 34] Photograft polymerization of AA onto the surface of PP film took place when the radical initiator BP into the reaction mixture was activated under UV-light effect. The activated BP was incorporated into the PP chain after abstracting hydrogen atom, starting AA polymerization (Figure 9). A typical G curve has an S-shaped against the reaction time, where a first induction period with a comparatively low G value is exhibited. Later, grafting increased rapidly in an intermediate stage. After that, the grafting rate decreased at a given reaction time and the reaction yield leveled off.[16, 33, 34] Clearly, this behavior agrees with that of the curve profile found in Figure 8, which supports the use of LDR sensor to control AA-photograft polymerization. We propose that this simple and inexpensive device can optimize photoluminous reaction conditions, which will lead to a more controlled grafting reaction with reproducible G values.

Figure 9

3.3 Relation between ignition time of lamp and G value

Grafting reactions were carried out at different stabilization times (t_1= 0, 2, 4, 6, 8, 10 and 15 min) after turning on the lamp, while for all cases an exposure time of 2 min was used. Lamp was covered with an opaque surface during stabilization time. Figure 10 shows that G value rapidly increased when stabilization time was less than 4 min. However, G value did not significantly change for a further time and reached its maximum value (G_{max}). This behavior was similar to that observed at least for the first period when conductance against the stabilization time of lamp was examined (Figure 8). A value of received dose (Dose) by the PP-RM-glass system from UV lamp for 2 minutes could be estimated using Equation 4:

$$\frac{Dose}{Dose_{\infty}}/a.u. \propto \int_{t_1}^{t_1+2} \frac{C_t}{C_{\infty}} dt \qquad (4)$$

where a definite integral of normalized conductance goes from t_1 to t_1+2 time. Figure 10 shows that the curve profile of Dose agrees with that of the G value for the different stabilization times analyzed. This phenomenon supports a clearly dependence between both parameters as a function of the stabilization lamp time. In addition, Dose and G value reached the highest value after a stabilization time around 4 min. This tendency is related to the fact that after the stabilization time reported above the lamp gives its maximum value of light intensity from which the performance of grafting reaction begins to depend on the reaction kinetics as well as on the transport phenomenon in the reaction mixture.

Figure 10

3.4 UV light variation against position of film into the reaction camera

Figure 11 shows the variation of the UV lamp recorded as a conductance value from the LDR sensor at different distances (A, B, C and D level). The blue spheres represent the points measured and the red dots denote the Gaussian adjustment from the data. In Figure 11 A, the LDR sensor was placed at 4 cm (A) from the lamp where conductance as a width function was examined. At this level, a large variation of conductance value is observed for different width values, where the central zone with a conductance value near 1.2 mS is 10 times higher than that found in peripheral areas. In the latter light scarcely comes, which can be seen from a weak conductance obtained. Figure 11 B shows that level B has a curve profile similar to that in level A, although the highest B conductance is 20 % lower than that found for A. In addition, the lateral B zones present a conductance higher than that found in Figure A. This performance highlights that a more homogeneous conductance value is reached when a longer distance to the lamp is used. Figure 11C shows that the conductance of C central area is 60 % in relation to maximum A level, and 6 times higher than that in its periphery area. In addition, Figure 11 D displays the conductance variation when the sensor was positioned in level D. It is found that the lowest conductance difference between the center and the periphery area is about 4 times. The differences seen in each level are attributed to the fact that the irradiance received by the sensor surface varies with the cosine of the angle between the direction of the UV light beam and the normal direction of the surface. This behavior agrees with that established by the Lambert law of the cosine where a peripheral zone has a large incidence angle, leading to a lower irradiance value. In addition, for a given level, if the sensor is placed on a more centered position under the light source, a smaller angle is reached, yielding a higher conductance value since the sensor position is already normal to the light source.

Figure 11

3.5 Effect of film position on the grafting reaction. Characterization of modified films

Grafting reactions were performed onto the surface of PP films using different distances from light source and several width positions for a given level. A lamp stabilization time of 8 min was used to reach a constant conductance before exposing the PP/RM/glass system to UV-light for 2 min. Figure 12 shows the G value and the conductance value as a position function of the PP film into the reactor, while the average conductance value and its standard deviation have been obtained from Figure 11. In all cases, it is observed that both central width positions (21 and 27 cm) have the highest G value, which agrees with the performance found for the conductance. This phenomenon is related to the fact that the highest irradiance value is achieved for these width positions (Figure 11). Figure 12 also shows that level A has the highest intensity variation, which yields the greatest G value with a value near 18 wt.-% for two central width zones. A similar tendency is found for level B with values slightly lower than those found in level A. However, levels C and D show an average G value of 13 and 10 wt.-%, respectively, since they are further away from the light source (Figure 12). It should be noted that a longer distance of film from the light source leads to a lower variation of both parameters against the width, which indicates that a more reproducible assay is obtained.

Figure 12

Considering the kind of reaction carried out during the photograft reaction of acrylic acid, the superficial modification of films could be demonstrated by FTIR-ATR spectrometry. Figure 13A shows the profile of the FTIR-ATR curves for the initial PP and the modified film at a given distance from the lamp. Clearly the profile of PP spectral curves varies substantially from the superficial modification of PP films. We can see characteristic bands of initial PP film such as the vibration mode for C-H stretching of methylene, methyl and methine group near 2960 and 2850 cm^{-1}, and C-H bending band corresponding to the methyl group close to 1387 cm^{-1}. Those bands decreased when a higher grafting degree of polyacrylic acid onto film surface was

reached, while a new signal at 1710 cm^{-1} attributed to the C=O stretching vibration of the carboxyl group was evidenced. The grafting degree attained could also be evaluated from the study of the band ratio corresponding to the signal of carbonyl group at 1710 cm^{-1} and the bending band of methyl group at 1387 cm^{-1}. Figure 13B shows that the band ratio 1710/1387 of the modified film surface at level A has a higher value than that observed for modified PP surface at level D. This behavior supports the fact that a lower distance leads to a higher grafting degree. Moreover, a higher variation of the band ratio can be found between the central and external position of the film along the lamp. The highest grafting degree was achieved in the central reactor zone, which changed substantially in relation to a lower value found at their external positions. However, when a longer distance from the UV lamp was used for PP film modification, its band ratio 1710/1387 slightly varied for different bandwidths evaluated, supporting the fact that a more homogeneous AA-photograft polymerization onto surface took place.

Figure 13A, B

Finally, the modification reaction onto PP surface was characterized through the study of the contact angle. Figure 14A shows the contact angle measurements of samples modified at levels A and D, determined by the Sessile Drop method. Samples of level D have a higher contact angle than those found for level A, since the higher grafting degree reached for the latter shows a better wettability. Moreover, it should be noted that the samples of level A show greater variability in the contact angle than that found in level D, which agrees with the high variation of intensity of UV light determined as conductance for the former. Subsequently, the thickness of the initial polypropylene and those modified films at levels A and D was compared. Figure 14B shows that the modified films at a shorter distance from the UV lamp present an average thickness value higher than that found for films modified at a longer distance. The latter have an

average thickness and uncertainty very close to that determined for initial PP film, despite having a grafting value close to 8 wt.-%, which shows a surface with a high homogeneity after the modification process. Clearly this behavior agrees with the variation of the previously analyzed light power (Figure 11), where the central zone has the highest light intensity. This phenomenon is related to the fact that the photograft reaction kinetics of acrylic acid directly depends on the UV radiation received by the system. Therefore, a higher G value is associated with a modified PP film with a greater PAA thickness and a surface more hydrophilic than that found for PP.

Figure 14 A, B

The results described above support the relationship found between the Dose and the G value, which can be calculated from conductance (Eq. 4). Therefore, the dose received will be proportional to the product of conductance by exposure time. Figure 15 shows the profile of the G curve as a conductance function where its adjustment function exhibits a linear correlation. Therefore, the G value (G_{est}) can be estimated from the following equation:

$$G_{est}/wt.-\% = (2.2 \pm 0.1)10^4 \; c - (0.3 \pm 0.4) \quad (5)$$

where a determination coefficient of 0.97 is obtained. This equation is useful at different levels and width positions of the PP film into the chamber from the conductance value. Figure 15 also shows that the G value has a lower uncertainty when a lower conductance is measured. Therefore, this correlation reaches a more predictive performance of grafting reaction for that level with a longer distance from the light source.

Figure 15

It is known that the radiant intensity is inversely proportional to the square of the distance from the source according to the inverse square law. Therefore, it can be estimated that the irradiance of the UV light received by the film at centered width positions decreases about 50 times from levels A to D, while the average G value goes from 18 to 8 wt.-%. Under these conditions, the average conductance is found to also decrease from near 9 to 4 mS, exhibiting a linear response against the G value, as shown in Figure 15. This behavior supports the fact that LDR conductance is a useful tool sensor to control photochemical reactions.

Conclusion

In this work, a photoconductive sensor (LDR) is used to determine the stabilization period of emission light from an UV lamp and the irradiance distribution measured as conductance into a reaction chamber, since both parameters have effect on the performance of the photochemical reaction. Different variables such as the position from lamp and its stabilization time were studied using a reaction model based on AA-photograft polymerization onto the surface of PP films. A relative sensitivity in the UV range was determined from the conductance measured with the LDR sensor, which was linked with the emitted light as a time function. It is found that light intensity as well as G value versus stabilization time describe a curve profile which agrees with a sigmoidal function, whose initial variation is related to the delay time of the lamp to reach thermal equilibrium. After 4 min, the light intensity achieves a maximum value, which keeps constant against time. This phenomenon is associated with a constant amount of Dose received by the PP-MR-glass system for a given position. Then, grafting performance depends only on reaction kinetics and transport phenomena. In addition, the average G value and its standard deviation decrease when the film is placed at a longer distance from the lamp. This phenomenon supports the fact that the irradiance received by the reaction mixture at a remote level has a more homogeneous light intensity, yielding a lower standard deviation of the G

value. This is a valuable result since a higher reproducibility of the G value can be estimated. In addition, the use of CdS sensor for AA-photograft polymerization could be validated as a simple and inexpensive device. Therefore, we propose to use of LDR as a useful sensor, which has demonstrated to be successful in monitoring the performance of lamp for UV-induced reaction.

Acknowledgements

María Fernanda Stragliotto, PhD., thanks CONICET for her postdoctoral fellowship. In addition, the authors are grateful for the financial support received by CONICET from the projects PIP 11220110100499CO and PIP 11220150100344CO, FONCYT (PICT-2015-2477) and SECYT-UNC (30820150100348CB). The authors also wish to acknowledge language assistance by Prof. Carolina Mosconi.

References

(1) Aranguren, P.; Roch, A.; Stepien, L.; Abt, M.; von Lukowicz, M.; Dani, I.; Astrain, D. Optimized design for flexible polymer thermoelectric generators. *Appl. Therm. Eng.* **2016**, 102, 402-411. DOI: 10.1016/j.applthermaleng.2016.03.037.

(2) Shi, Y.; Jiang, R.; Liu, M.; Fu L.; Zeng, G.; Wan, Q.; Mao, L.; Deng, F.; Zhang, X.; Wei, Y. Facile synthesis of polymeric fluorescent organic nanoparticles based on the self-polymerization of dopamine for biological imaging. *Mat. Sci. Eng. C*. **2017**, 77, 972-977. DOI: 10.1016/j.msec.2017.04.033.

(3) Therkorn, J.; Thomas, N.; Calderón, L.; Scheinbeim, J.; Mainelis, G. Development of a Passive Bioaerosol Sampler using Polarized Ferroelectric Polymer Film. *J. Aerosol Sci.* **2017**, 105, 128-144. DOI: 10.1016/j.jaerosci.2016.12.002.

(4) Bhattacharya, P.; Shantini Ramasamy, U.; Krueger, S.; Robinson, J.W.; Tarasevich, B.J.; Martini, A.; Cosimbescu. L. Trends in Thermoresponsive Behavior of Lipophilic Polymers. *Ind. Eng. Chem. Res.* **2016**, 55, 12983-12990. DOI: 10.1021/acs.iecr.6b03812.

(5) Brooke, R.; Fabretto, M.; Murphy, P.; Evans, D.; Cottis, P.; Talemi, P. Recent advances in the synthesis of conducting polymers from the vapour phase. *Prog. Mater. Sci*. **2017**, 86, 127-146. DOI: 10.1016/j.pmatsci.2017.01.004.

(6) Aplan, M.P.; Gomez, E.D. Recent developments in chain-growth polymerizations of conjugated polymers. *Ind. Eng. Chem. Res.* **2017**, 56, 7888–7901. DOI: 10.1021/acs.iecr.7b01030.

(7) Kwon, O.H.; Nho, Y.C.; Chen, J. Surface Modification of Polypropylene Film by RadiationInduced Grafting and Its Blood Compatibility*. J. Appl. Polym. Sci*. **2003**, 88, 1726-1736. DOI: 10.1002/app.11832.

(8) Song, Y.W.; Do, H.S.; Joo, H.S.; Lim, D.H.; Kim, S.; Kim, H.J. Effect of grafting of acrylic acid onto PET film surfaces by UV irradiation on the adhesion of PSAs.*J. Adhes. Sci. Technol.* **2006**, 20, 1357-1365. DOI: 10.1163/156856106778456564.

(9) Zheng, I.; Gurgel, P.V.; Carbonell, R.G. Effects of UV Exposure and Initiator Concentration on the Spatial Variation of Poly(glycidyl methacrylate) Grafts on Nonwoven Fabrics. *Ind. Eng. Chem. Res.* **2011**, 50, 6115-6123. DOI: 10.1021/ie1021333.

(10) Fernandez-Gutierrez, M.; Olivares, E.; Pascual, G.; Bellón, J.M.; San Román, J. Low-densitypolypropylene meshes coated with resorbable and biocompatible hydrophilic polymers ascontrolled release agents of antibiotics. *Acta Biomater.* **2013**, 9, 6006-6018. DOI: 10.1016/j.actbio.2012.12.012.

(11) Mandal, D.K.; Bhunia, H.; Bajpai, P.K.; Kushwaha, J.P.; Chaudhari, C.V.; Dubey, K.A.; Varshney, L. Optimization of acrylic acid grafting onto polypropylene using response surface methodology and its biodegradability. *Radiat. Phys. Chem.* **2017**, 132, 71-81. DOI: 10.1016/j.radphyschem.2016.12.003.

(12) Korolkov, I.V.; Güven, O.; Mashentseva, A.A.; Atıcı, A.B.; Gorin, Y.G.; Zdorovets, M.V.; Taltenov, A.A. Radiation induced deposition of copper nanoparticles inside the nanochannels of poly(acrylic acid)-grafted poly(ethylene terephthalate) track-etched membranes. *Radiat. Phys.Chem.* **2017**, 130, 480-487. DOI: 10.1016/j.radphyschem.2016.10.006.

(13) Balart, J.; Fombuena, V.; Balart, R.; España, J.M.; Navarro, R.; Fenollar, O. Optimization of Adhesion Properties of Polypropylene by Surface Modification Using Acrylic Acid Photografting. *J. Appl. Polym. Sci.* **2010**, 116, 3256-3264. DOI: 10.1002/app.31751.

(14) Kazmi, S.M.R.; Jayaraman, K.; Das, R. Single-step Manufacturing of Curved Polypropylene Composites Using a Unique Sheet Consolidation Method. *J. Mater. Process. Tech*. **2016**, 237,96–112. DOI: 10.1016/j.jmatprotec.2016.05.028.

(15) Riveiro, A.; Soto, R.; del Val, J.; Comesaña, R.; Boutinguiza, M.; Quintero, F.; Lusquiños, F.; Pou, J. Texturing of polypropylene (PP) with nanosecond lasers.*Appl. Surf. Sci.* **2016**, 374, 379-386. DOI: 10.1016/j.apsusc.2016.01.206.

(16) Cavallo, J.A.; Gomez, C.G.; Strumia, M.C. Formation of Poly(propylene)-Based Biocomposite Films and Their Use in the Attachment of Methylene Blue. *Macromol. Chem.Phys*. **2010**, 211, 1793-1802. DOI: 10.1002/macp.201000047.

(17) Cavallo, J.A.; Gomez, C.G.; Strumia, M.C. Preparation of a milk spoilage indicator adsorbedto a modified polypropylene film as an attempt to build a smart packaging. *J. Food Eng.* **2014**, 136, 48-55. DOI: 10.1016/j.jfoodeng.2014.03.021.

(18) Zhao, A.; Li, Z.; Wang, H. Acetone/Water as a new photoinitiating system for photografting: A theoretical study. *Polymer.* **2010**, 51, 2099-2105. DOI: 10.1016/j.polymer.2010.02.050.

(19) Mandal, D.K.; Bhunia, H.; Bajpai, P.K.; Chaudhari, C.V.; Dubey, K.A.; Varshney, L. Radiation induced grafting of acrylic acid onto polypropylene film and its biodegradability. *Radiat. Phys. Chem.* **2016**, 123, 37-45. DOI: 10.1016/j.radphyschem.2016.02.011.

(20) Domenichelli, I.; Coiai, S.; Pinzino, C.; Taddei, S.; Martinelli, E.; Cicogna, F. Polymer surface modification by photografting of functional nitroxides. *Eur. Polym. J.* **2017**, 87, 24-38. DOI: 10.1016/j.eurpolymj.2016.12.002.

(21) Xiong, X.; Liu, W.; Luan, Y.; Du, J.; Wu, Z.; Chen, H. A Versatile, Fast, and Efficient Method of Visible-Light-Induced Surface Grafting Polymerization. *Langmuir.* **2014**, 30, 5474-5480. DOI: 10.1021/la500983s.

(22) Xin, Z.; Du, S.; Zhao, C.; Chen, H.; Sun, M.; Yan, S.; Luan, S.; Yin, J. Antibacterial performance of polypropylene nonwoven fabric wound dressing surfaces containing passive and active components. *Appl. Surf. Sci.* **2016**, 365, 99-107. DOI: 10.1016/j.apsusc.2015.12.217.

(23) Zhou, T.; Zhu, Y.; Li, X.; Liu, X.; Yeung, K.W.K.; Wu, S.; Wang, X.; Cui, Z.; Yang, X.; Chu, P.K. Surface Functionalization of Biomaterials by Radical Polymerization. *Prog. Mater. Sci.* **2016**, 83, 191-235. DOI: 10.1016/j.pmatsci.2016.04.005.

(24) Shin, J.; Liu, X.; Chikthimmah, N.; Lee, Y.S. Polymer Surface Modification Using UV Treatmentfor Attachment of Natamycin and the Potential Applications for Conventional Food Cling Wrap (LDPE). *Appl. Surf. Sci*. **2016**, 386, 276-284. DOI: 10.1016/j.apsusc.2016.05.158.

(25) Tretinnikov, O.N.; Gorbachev, A.A.; Lutsenko, E.V.; Danilchik, A.V.; Shkrabatovskaya, L.V.; Prikhodchenko, L.K. Photoinduced Grafting Polymerization onto the Surface with the Use of Radiation of High-Power Ultraviolet Light-Emitting Diodes. *Polym. Sci. Ser. B.* **2016**, 58, 278-283. **DOI:** 10.1134/S1560090416030155.

(26) Decker, C.; Zahouily, K. Surface Modification of Polyolefins by Photografting of Acrylic Monomers. *Macromol. Symp*. **1998**, 129, 99-108. DOI: 10.1002/masy.19981290109.

(27) Li, W.; Li, M.; Bolton, J.R.; Qiang, Z. Configuration optimization of UV reactors for water disinfection with computational fluid dynamics: Feasibility of using particle minimum UV dose asa performance indicator.*Chem. Eng. J.* **2016**, 306, 1-8. DOI: 10.1016/j.cej.2016.07.042.

(28) Abdel-Galil, A.; Ali, H.E.; Balboul, M.R. (Photo) influence of CdS nano-additives on optical, thermal and mechanical performance of CdS/polyvinyl alcohol nanocomposites. *Optik.* **2017,**129, 153-162. DOI: 10.1016/j.ijleo.2016.10.061.

(29) Naranyana Swamy, T.N.; Shelke, A.R.; Lokhande, A.C.; Pushpalatha, H.L.; Lokhande, C.D.; Ganesha, R. (Photo) electrochemical studies of chemically deposited h-CdS thin films. *Optik.* **2017**, 138, 192-199. DOI: 10.1016/j.ijleo.2017.03.042.

(30) Alkuam, E.; Mohammed, M.; Chen, T.P. Fabrication of CdS nanorods and nanoparticles with PANI for (DSSCs) dye-sensitized solar cells.*Sol. Energy*. **2017**, 150, 317-324.DOI: 10.1016/j.solener.2017.04.056.

(31) Barboiu, V.; Avadanei, M.I. Chemical reactions of benzophenone photoirradiated in 1,2-polybutadiene. *J. Photoch. Photobio. A*. **2011**, 222, 170-179. DOI: 10.1016/j.jphotochem.2011.05.018.

(32) LDR 5 mm - Light Dependent Resistor - SUNROM (Electronics / Technologies). http://www.sunrom.com/p/ldr-5mm-light-dependent-resistor (accessed July, 2017).

(33) Francis, S.; Dhanawade, B.R.; Mitra, D.; Varshney, L.; Sabharwal, S. Radiation-induced grafting of diallyldimethylammonium chloride onto acrylic acid grafted polyethylene. *Radiat. Phys. Chem*. **2009**, 78, 42-47. DOI: 10.1016/j.radphyschem.2008.07.004.

(34) Lei, J.; Liao, X. Surface graft copolymerization of acrylic acid onto LDPE film through corona discharge. *Eur. Polym. J.* **2001**, 37, 771- 779. DOI: 10.1016/S0014-3057(00)00177-4.

LIST OF CAPTIONS

Figure 1. Diagram of acquisition system of the UV light.

Figure 2. Determination of UV response time of LDR using a micro-controlled stepper motor.

Figure 3. Different positions of the LDR sensor into the UV reaction camera.

Figure 4. 3D scheme shows the films position inside of reaction camera. These dots delimit the perimeter of 4 films for each level and a given width.

Figure 5. Centered position of the PP film into reaction camera used to analysis the time of lamp stabilization at the level C.

Figure 6. Spectral sensitivity (%) of the LDR sensor. Inset shows a zoom in on the sensitivity values around UV light range.

Figure 7. Conductance of the LDR sensor vs. time in absence and presence of UV light.

Figure 8. Normalized conductance ($C_{254}.C_{\infty}^{-1}$) vs. time after turning on the lamp. Error bars show the standard deviations of measurements. The red line shows the adjustment obtained from the Equation 3.

Figure 9. Mechanism proposed for photograft polymerization of AA onto the surface of PP.

Figure 10. Grafting degree (sphere) and the Dose value (star) versus stabilization time (t_1) after turning on UV light source for level C.

Figure 11. Effect of the position of LDR on the conductance, at different distances from the lamp source (levels A, B, C and D). The blue spheres are the measured points and the red dots correspond to the Gaussian adjustment of the data.

Figure 12. Effect of the film position on the grafting reaction (black circle) versus the width value. Average conductance determined from Figure 11 (red circle) for levels A, B, C and D.

Figure 13A. FTIR-ATR spectra of the initial PP (black) and the modified film of level D (red).

Figure 13B. FTIR-ATR. Band ratio 1710/1387 corresponding to modified PP films attained at A (red square) and level D (blue square).

Figure 14A. Contact angle of the surface of modified films for A (red circle) and level D (black circle).

Figure 14B. Thickness of initial PP film (black circle) and modified films for A (red square) and level D (blue square).

Figure 15. The G value as a conductance function together with its adjustment curve.

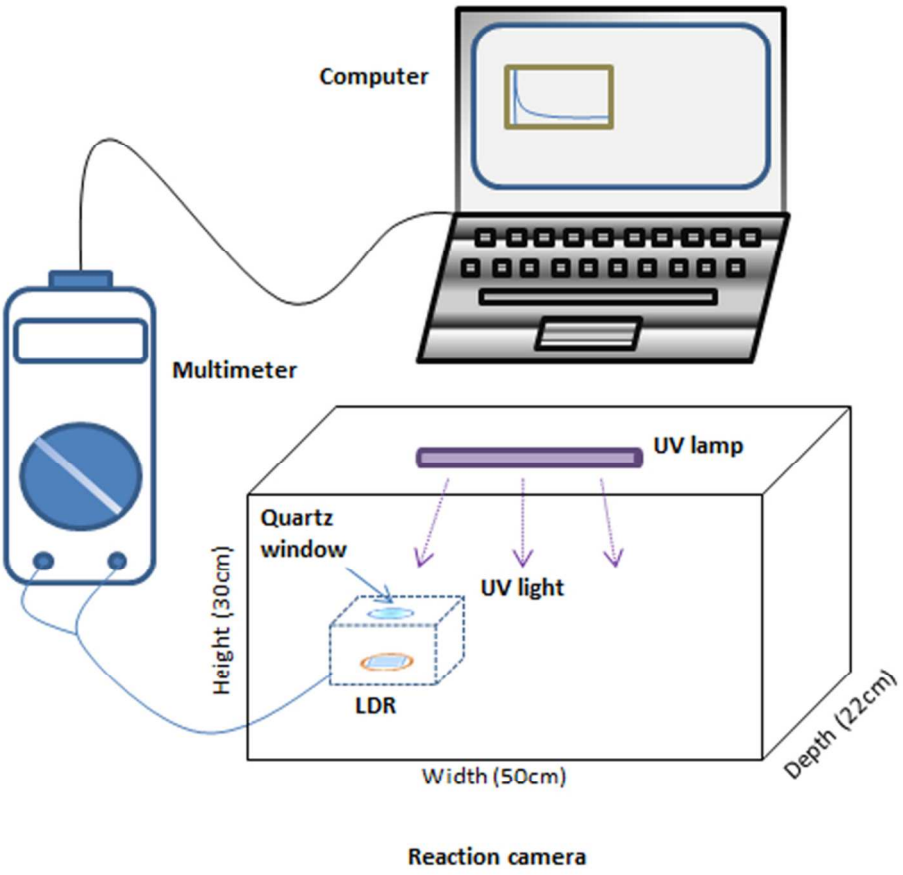

Figure 1. Diagram of acquisition system of the UV light.

34x32mm (600 x 600 DPI)

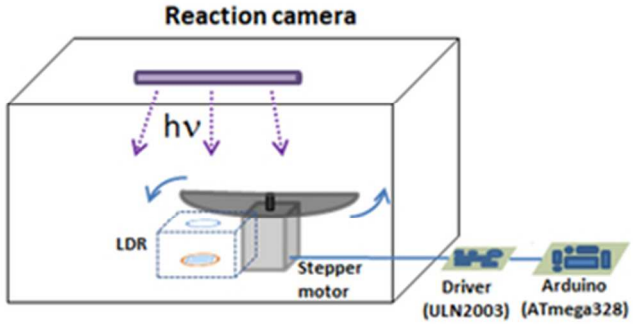

Figure 2. Determination of UV response time of LDR using a micro-controlled stepper motor.

14x7mm (600 x 600 DPI)

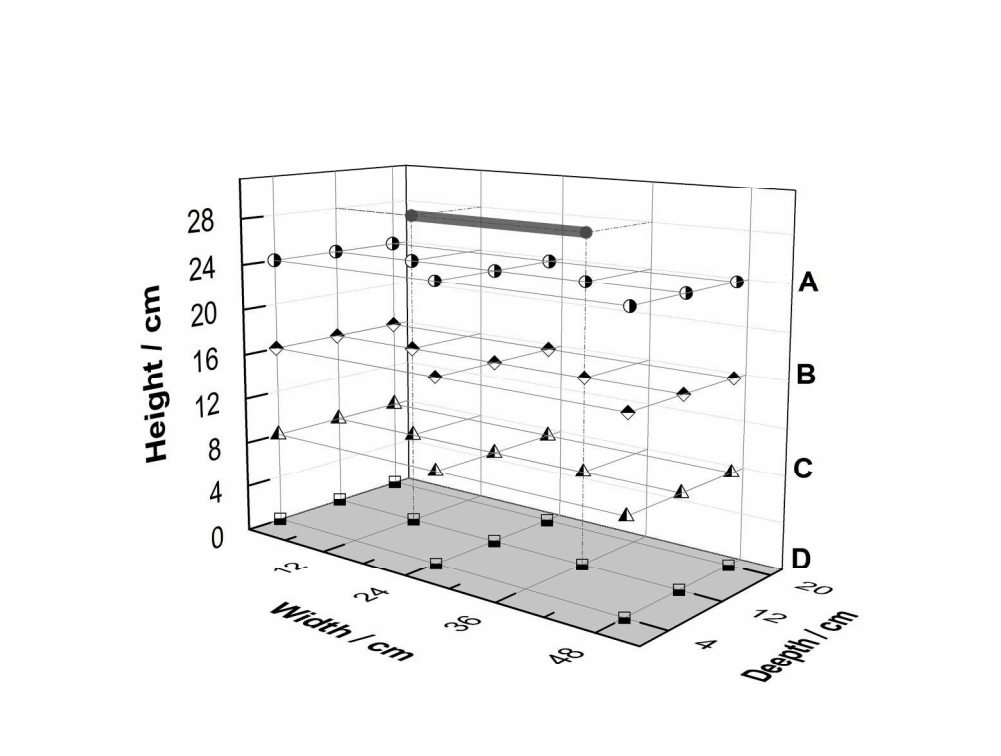

Figure 3. Different positions of the LDR sensor into the UV reaction camera.

205x156mm (300 x 300 DPI)

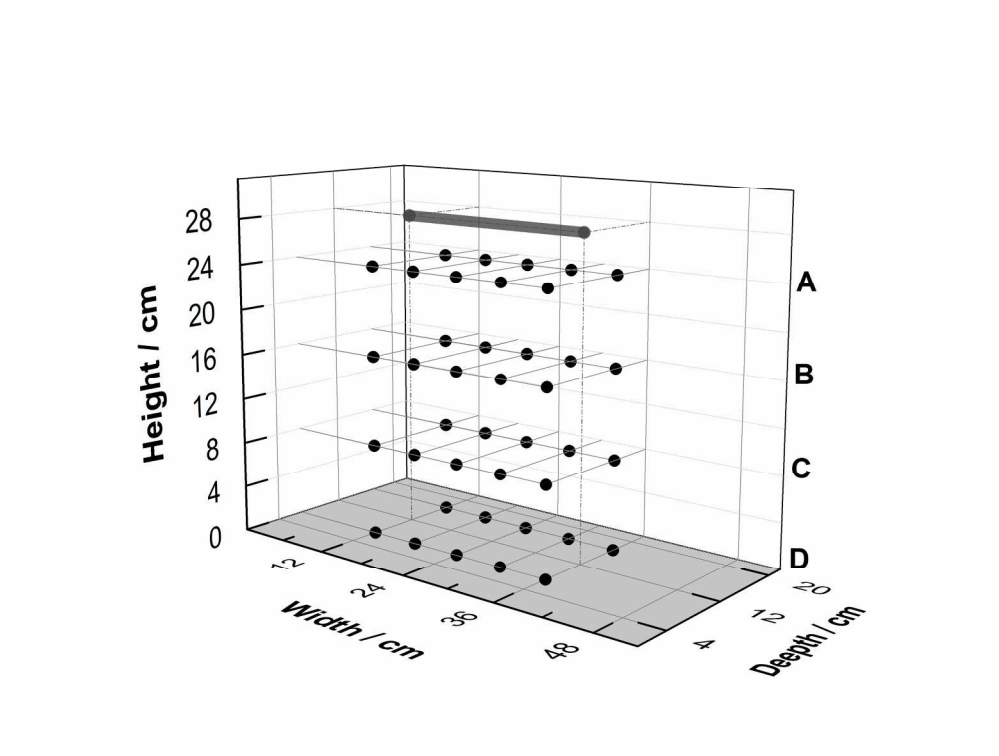

Figure 4. 3D scheme shows the films position inside of reaction camera. These dots delimit the perimeter of 4 films for each level and a given width.

205x156mm (300 x 300 DPI)

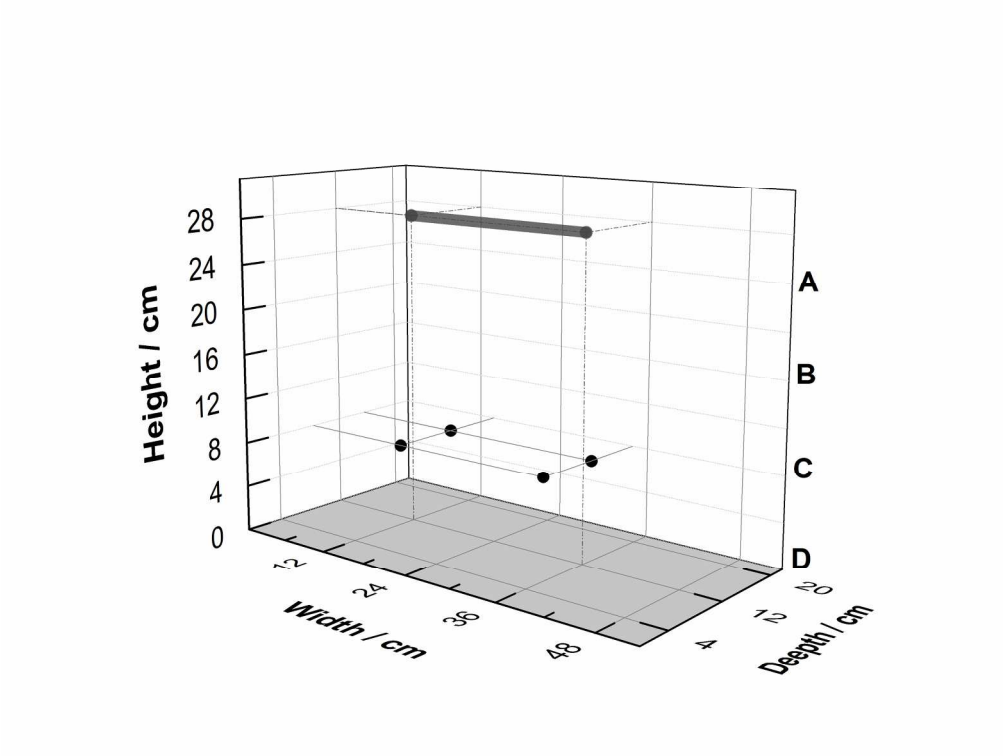

Figure 5. Centered position of the PP film into reaction camera used to analysis the time of lamp stabilization at the level C.

205x156mm (300 x 300 DPI)

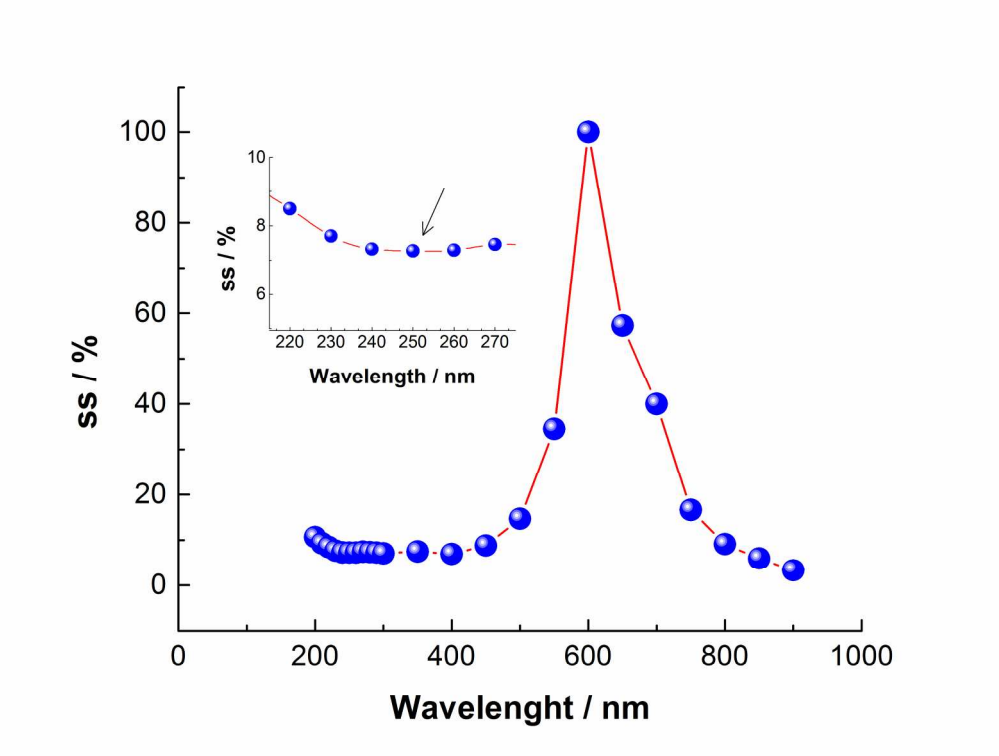

Figure 6. Spectral sensitivity (%) of the LDR sensor. Inset shows a zoom in on the sensitivity values around UV light range.

205x156mm (300 x 300 DPI)

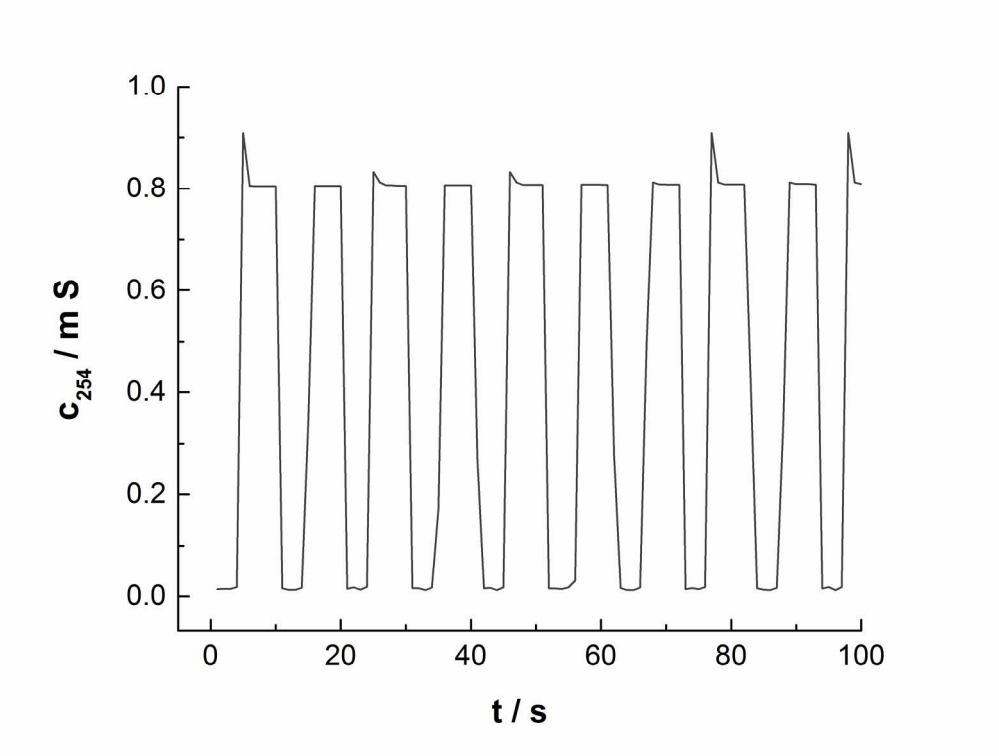

Figure 7. Conductance of the LDR sensor vs. time in absence and presence of UV light.

205x156mm (300 x 300 DPI)

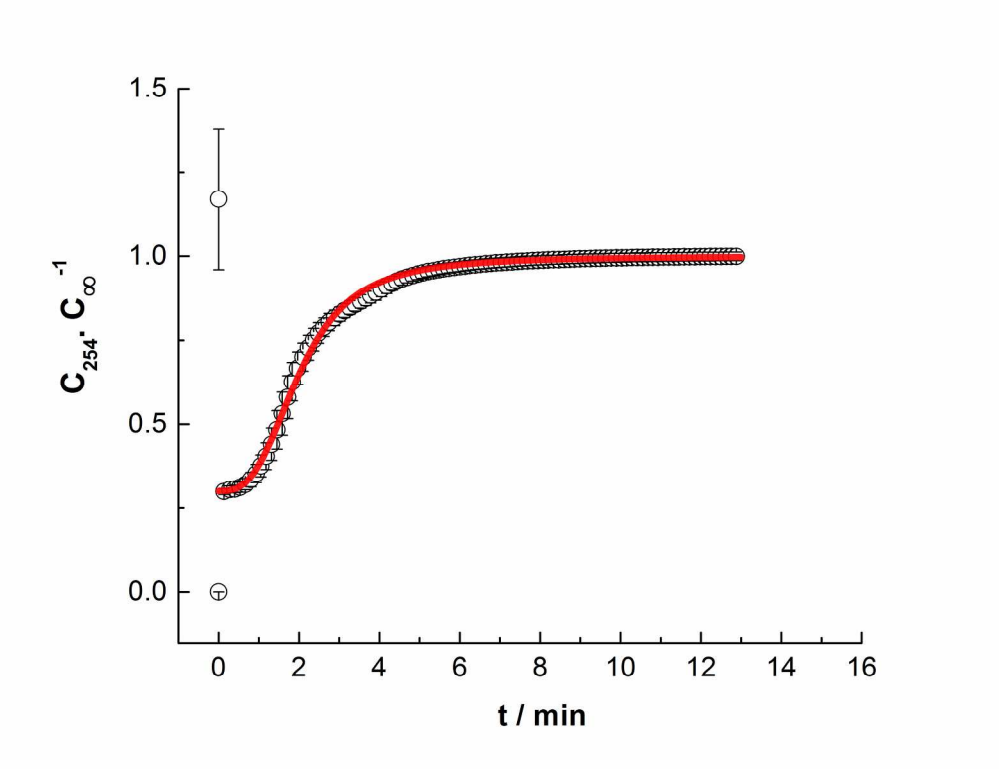

Figure 8. Normalized conductance (C254.C∞-1) vs. time after turning on the lamp. Error bars show the standard deviations of measurements. The red line shows the adjustment obtained from the Equation 3.

215x166mm (300 x 300 DPI)

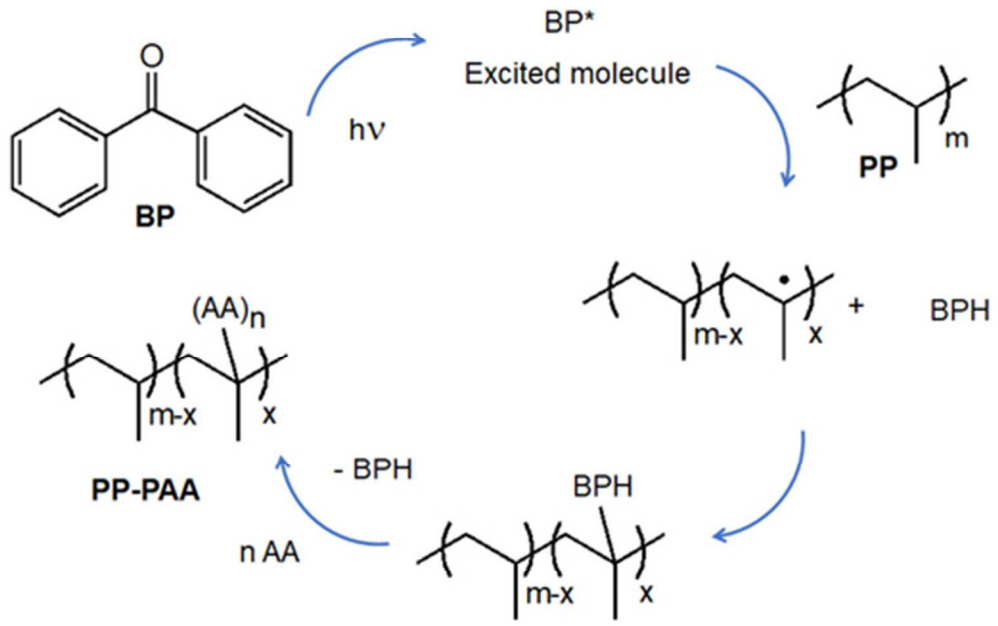

Figure 9. Mechanism proposed for photograft polymerization of AA onto the surface of PP.

44x33mm (300 x 300 DPI)

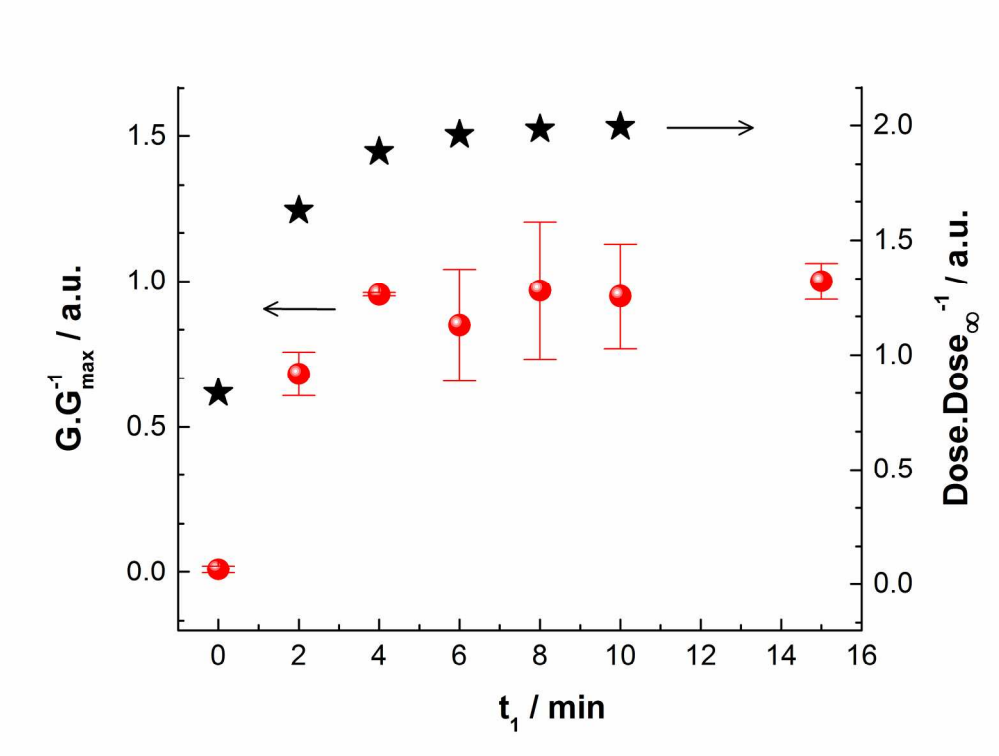

Figure 10. Grafting degree (sphere) and the Dose value (star) versus stabilization time (t1) after turning on UV light source for level C.

205x156mm (300 x 300 DPI)

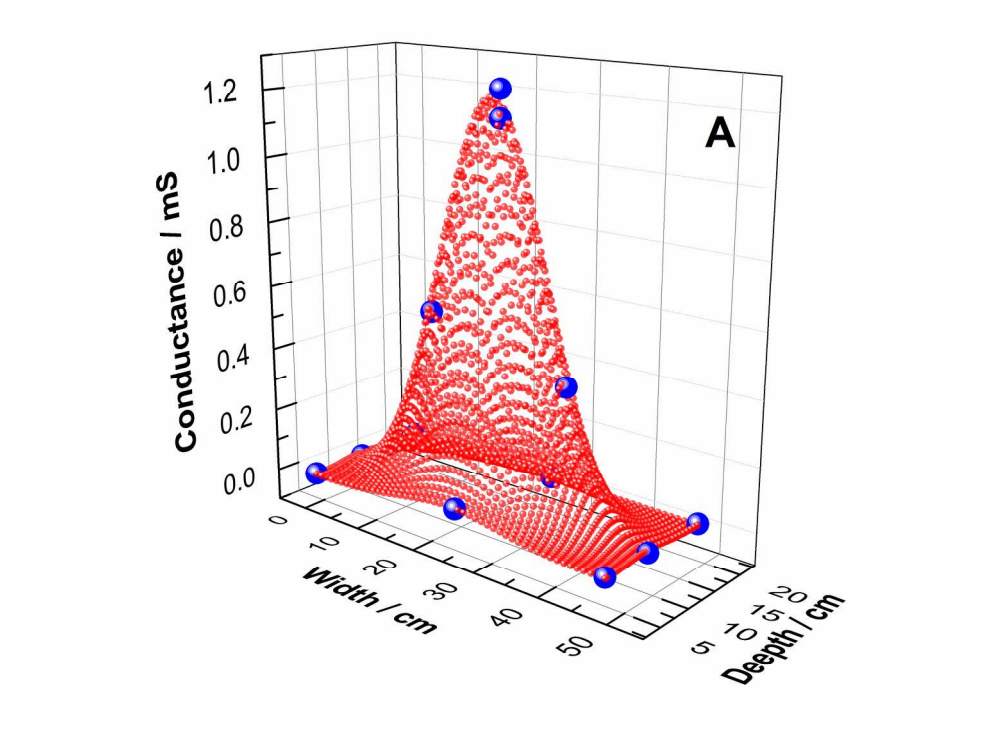

Figure 11. Effect of the position of LDR on the conductance, at different distances from the lamp source (A, B, C and D level). The blue spheres are the measured points and the red dots correspond to the Gaussian adjustment of the data.

205x156mm (300 x 300 DPI)

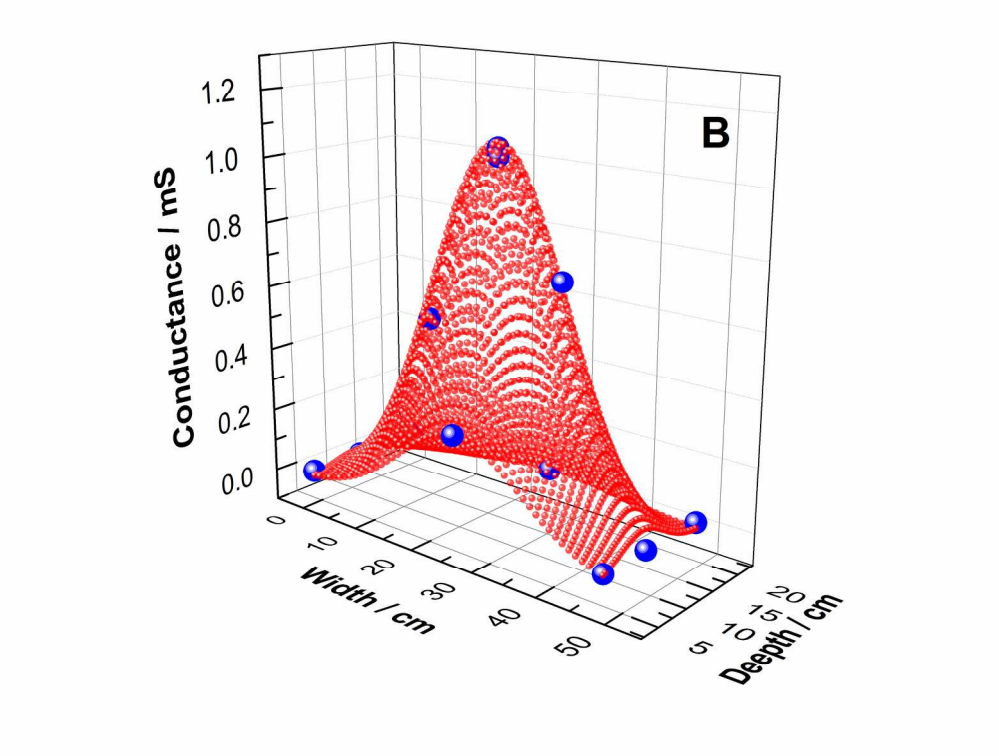

Figure 11. Effect of the position of LDR on the conductance, at different distances from the lamp source (A, B, C and D level). The blue spheres are the measured points and the red dots correspond to the Gaussian adjustment of the data.

205x156mm (300 x 300 DPI)

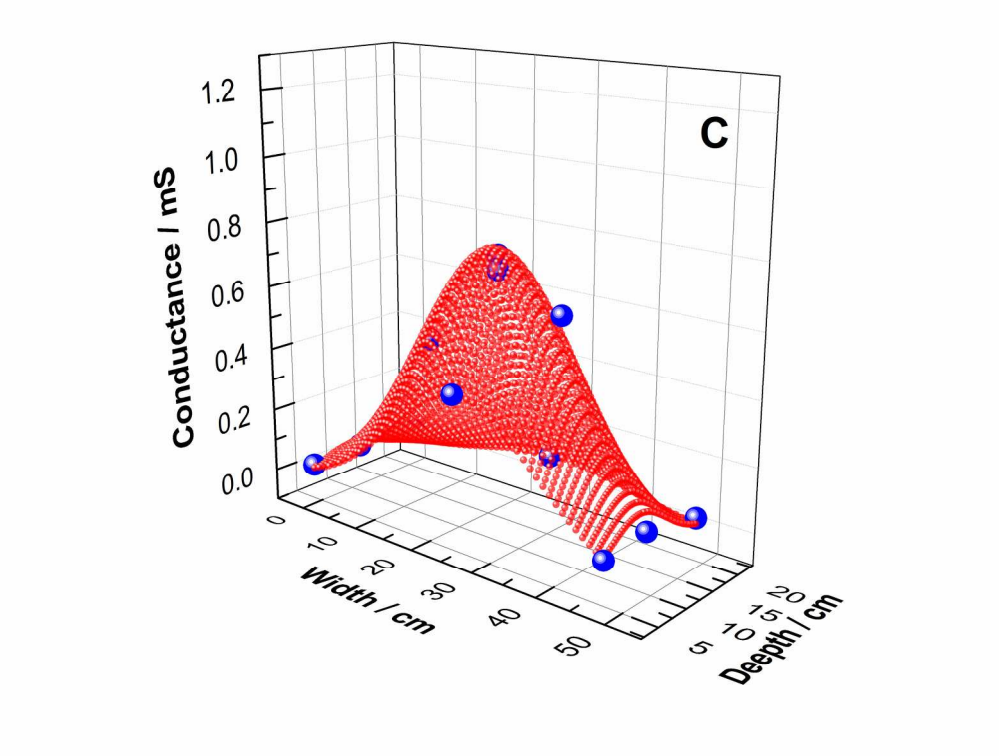

Figure 11. Effect of the position of LDR on the conductance, at different distances from the lamp source (A, B, C and D level). The blue spheres are the measured points and the red dots correspond to the Gaussian adjustment of the data.

205x156mm (300 x 300 DPI)

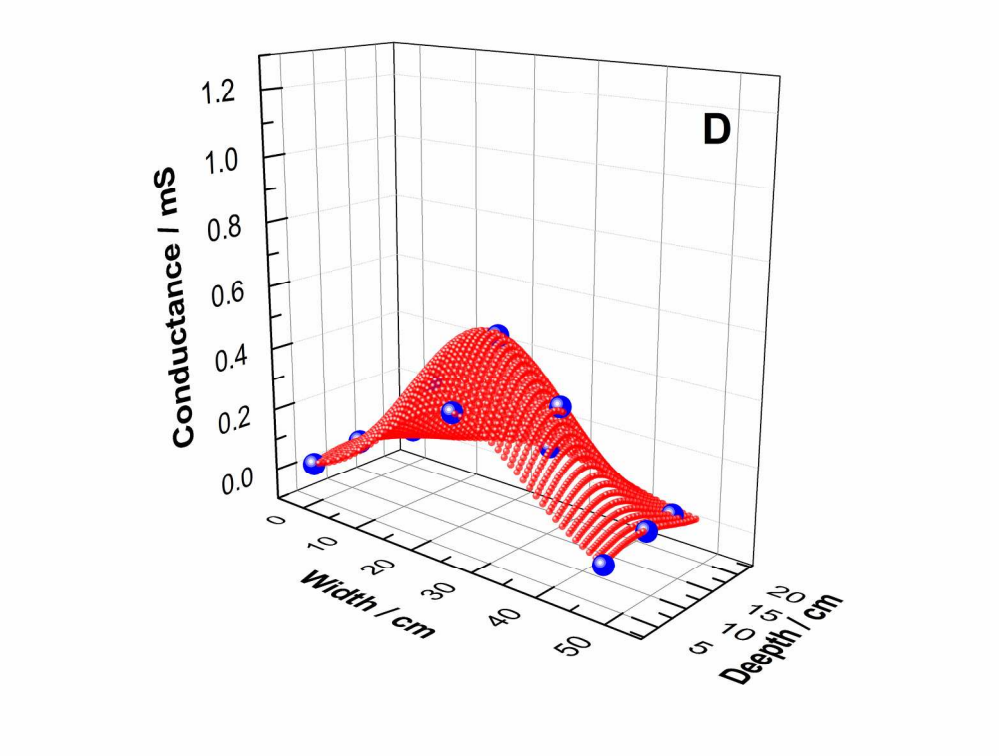

Figure 11. Effect of the position of LDR on the conductance, at different distances from the lamp source (A, B, C and D level). The blue spheres are the measured points and the red dots correspond to the Gaussian adjustment of the data.

205x156mm (300 x 300 DPI)

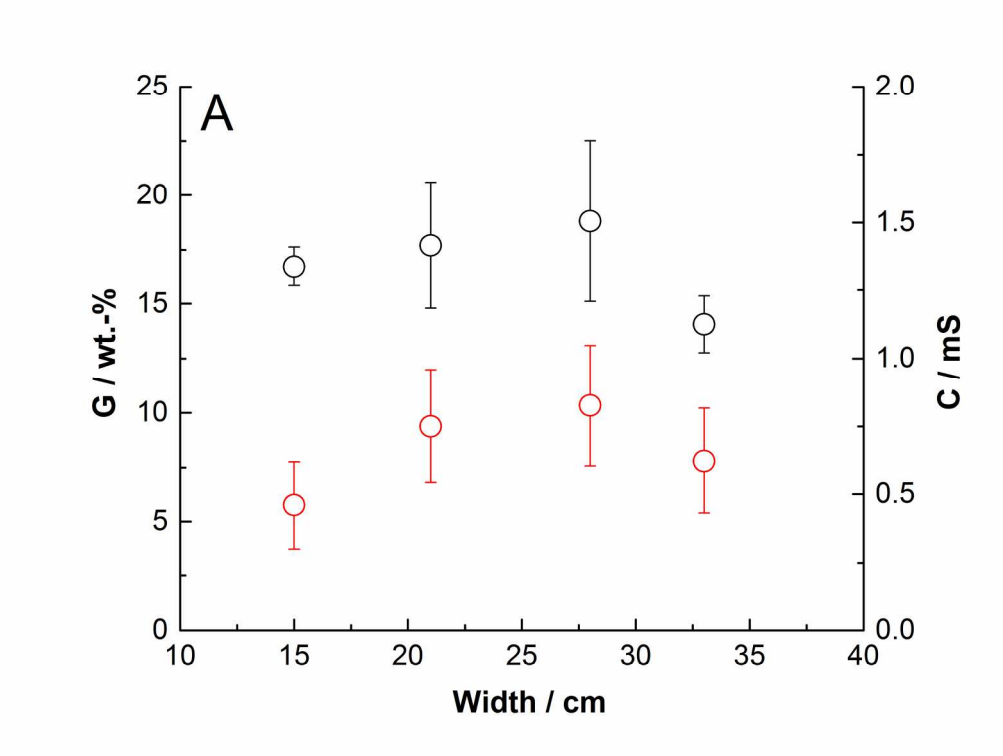

Figure 12. Effect of the film position on the grafting reaction (black circle) versus the width value. Average conductance determined from Figure 11 (red circle) for A, B, C and D level.

205x156mm (300 x 300 DPI)

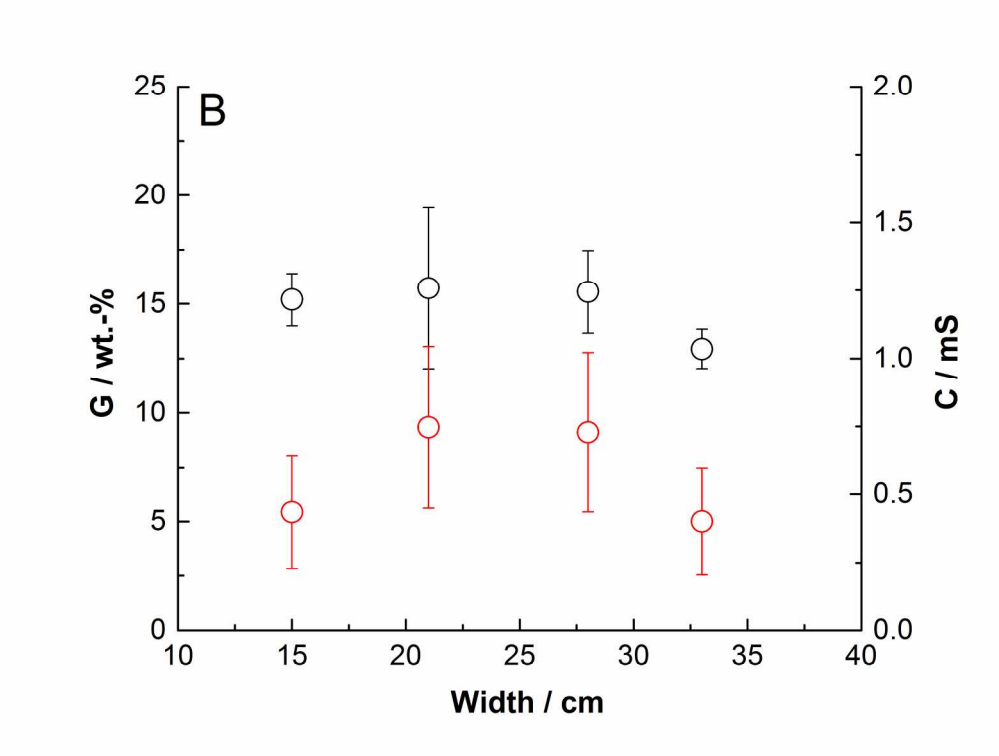

Figure 12. Effect of the film position on the grafting reaction (black circle) versus the width value. Average conductance determined from Figure 11 (red circle) for A, B, C and D level.

205x156mm (300 x 300 DPI)

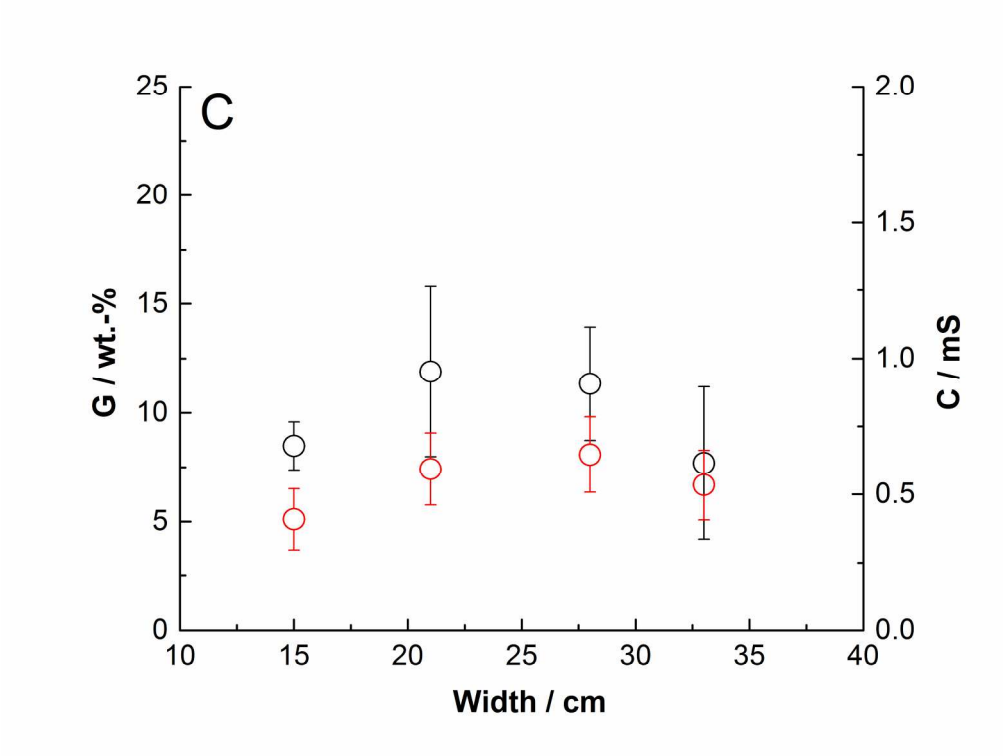

Figure 12. Effect of the film position on the grafting reaction (black circle) versus the width value. Average conductance determined from Figure 11 (red circle) for A, B, C and D level.

205x156mm (300 x 300 DPI)

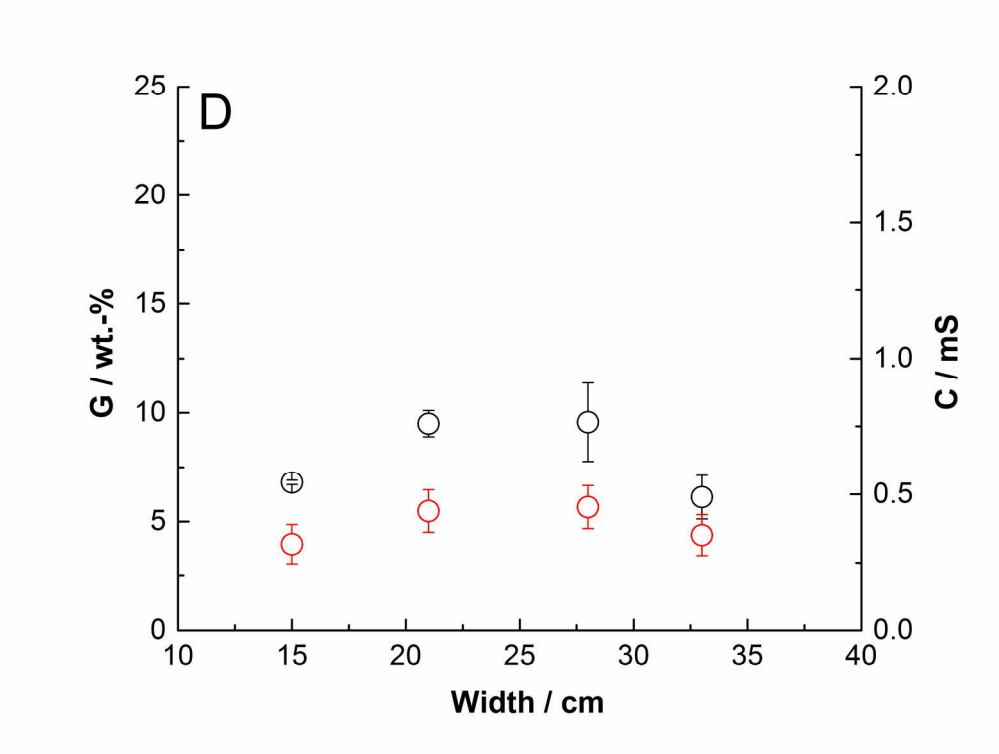

Figure 12. Effect of the film position on the grafting reaction (black circle) versus the width value. Average conductance determined from Figure 11 (red circle) for A, B, C and D level.

205x156mm (300 x 300 DPI)

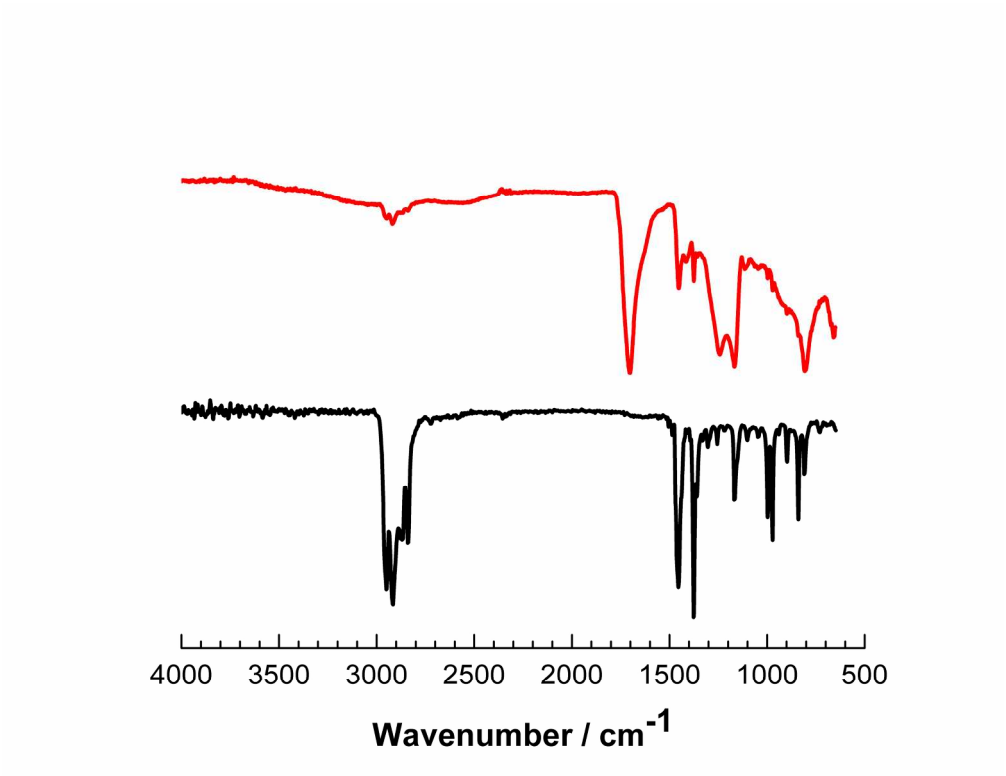

Figure 13A. FTIR-ATR spectra of the initial PP (black) and the modified film of level D (red).

210x162mm (300 x 300 DPI)

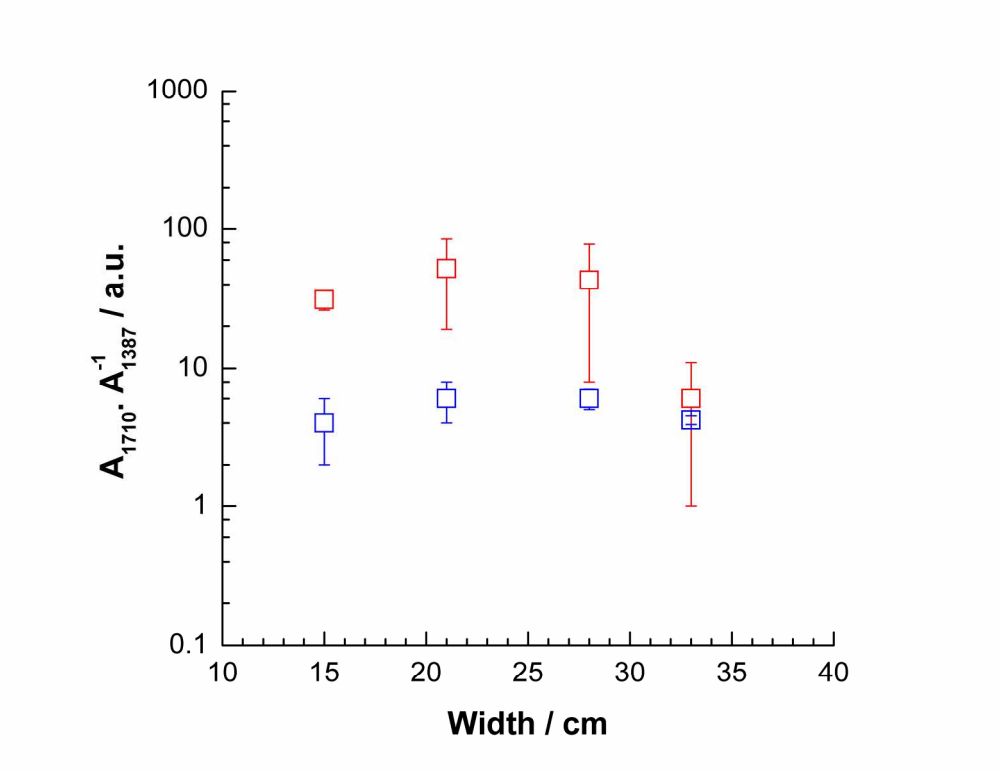

Figure 13B. FTIR-ATR. Band ratio 1710/1387 corresponding to modified PP films attained at A (red square) and D level (blue square).

210x162mm (300 x 300 DPI)

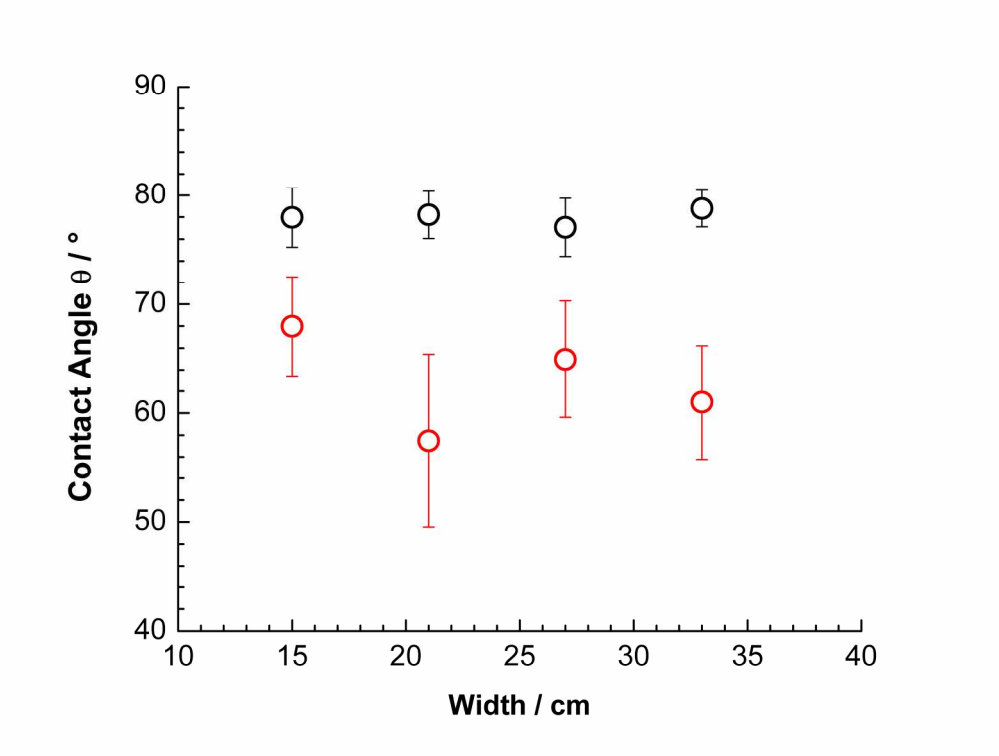

Figure 14A. Contact angle of the surface of modified films for A (red circle) and D level (black circle).

206x156mm (300 x 300 DPI)

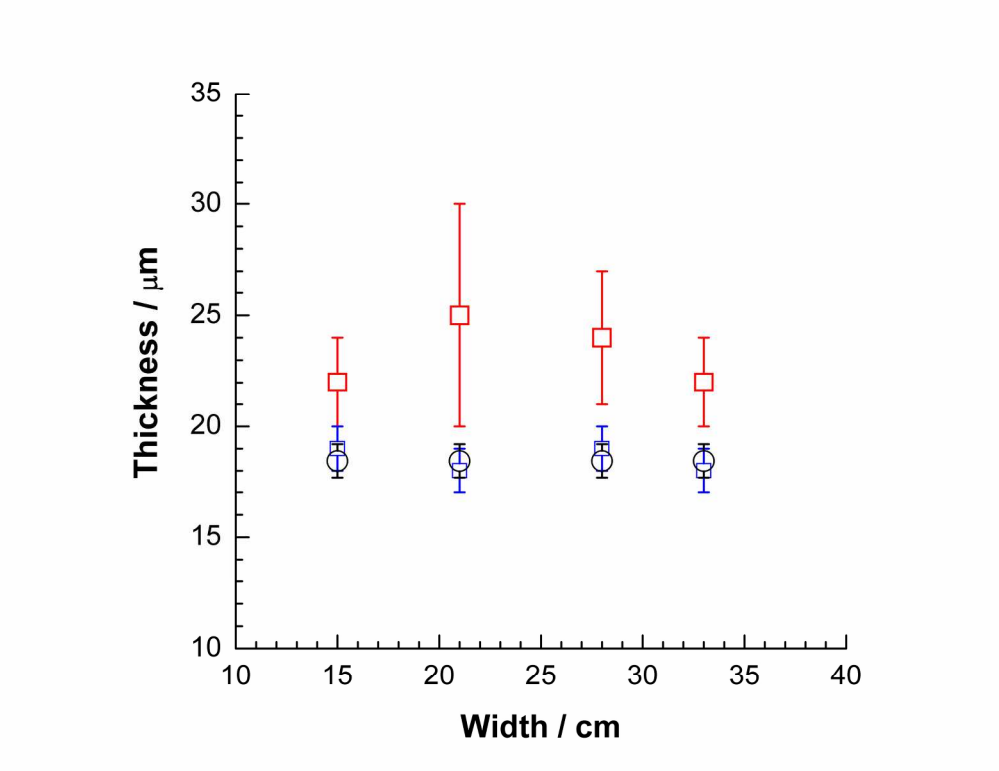

Figure 14B. Thickness of initial PP film (black circle) and modified films for A (red square) and D level (blue square).

210x162mm (300 x 300 DPI)

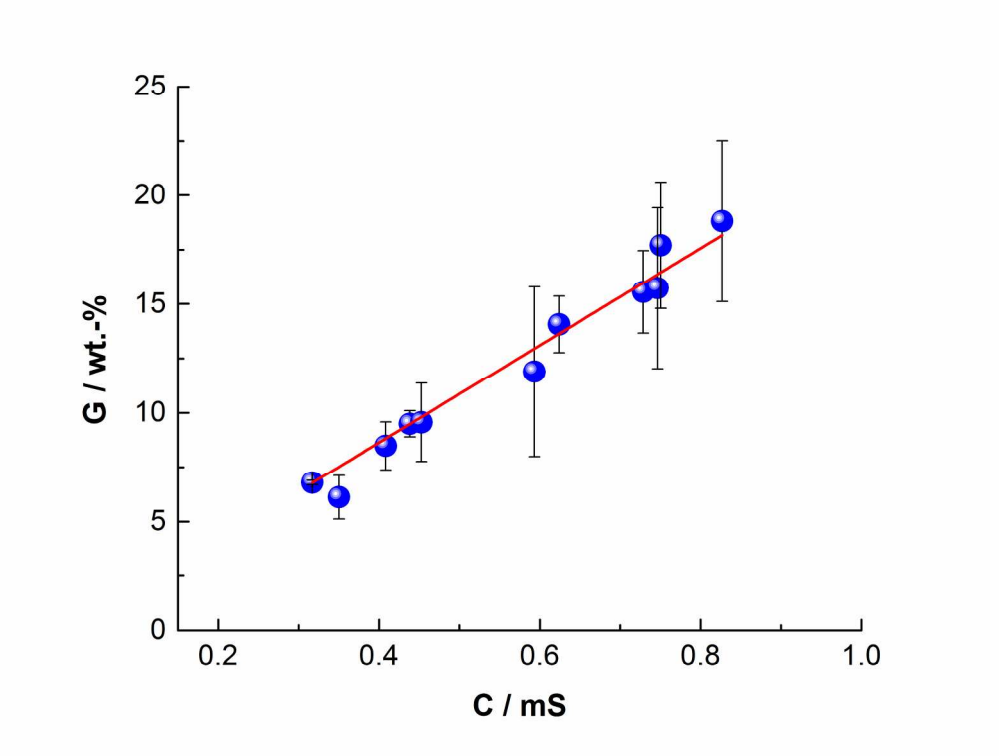

Figure 15. The G value as a conductance function together with its adjustment curve.

205x156mm (300 x 300 DPI)

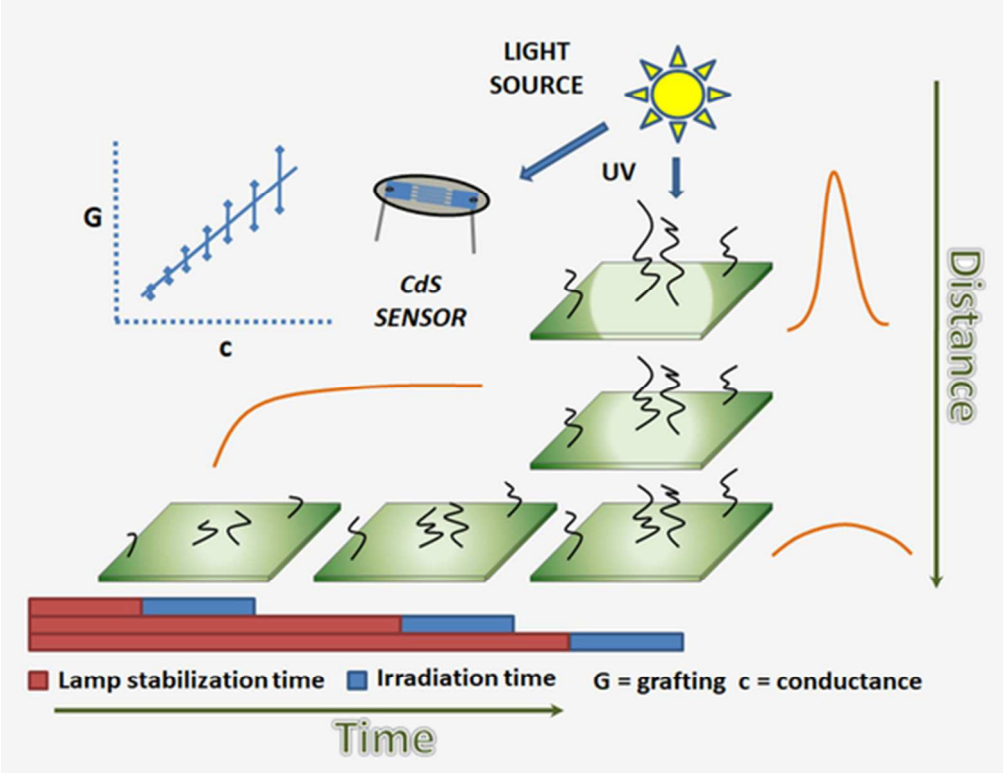

48x37mm (300 x 300 DPI)